ION THRUSTER THRUST VECTORING BY GRID TRANSLATION

Yasushi Okawa*, Yukio Hayakawa†, Katsuhiro Miyazaki†, and Shoji Kitamura†

* Japan Society for the Promotion of Science
† National Aerospace Laboratory of Japan

Three-dimensional and two-dimensional Particle-in-Cell simulation codes were developed to calculate the ion beam deflection phenomena by grid translation in ion thrusters. Beamlet behavior in ion optics with ordinal circular apertures and slit apertures was simulated using these codes. The results indicated that 1) a beam deflection angle is proportional to a grid offset angle and the inclination strongly depends on the number density of discharge-chamber plasma, 2) the grid displacement direction with reference to grid aperture arrangement has slight influences on beam deflection capability, 3) a larger beam deflection angle is obtained by slit apertures than ordinal ones. The obtained results are useful to design the ion optics with grid translation mechanisms for thrust vector control.

1. Introduction

The thrust vector control of ion thrusters by means of ion beam deflection in ion optics is an attractive way to enhance the capability of ion thrusters. This thrust vectoring mechanism dispenses with conventional gimbaling devices and reduces propulsion system mass. Since 1960's, some experimental and numerical studies[1-6] have been performed concerning the ion beam deflection for thrust vector control. Some methods have been contrived to deflect an ion beamlet, such as grid translation, electrostatic field application, electromagnetic field application and divided electrode insertion.[1] In these options, the grid translation method has been examined vigorously because it is the simplest both in theory and practice. Figure 1 depicts the schematic of beamlet deflection phenomenon by grid translation. An ion beamlet is deviated by displacing an accelerator grid laterally with reference to thrust axis. The definitions of a grid displacement distance ε, a grid offset angle δ, and a beamlet deflection angle β follow the descriptions in the report by Homa and Wilbur.[4]

The basic theory and mechanism on the beam deflection by grid translation had been well-developed in the studies above. However, its application to on-orbit flight has not been accomplished due to some reasons, such as the thermal expansion problem of metal electrodes and the reliability of grid translation mechanisms. In these problems, the thermal expansion of metal electrodes is probably the most important one. If the metal materials such as molybdenum are used, dished grids are necessary to maintain the grid-to-grid separation. In

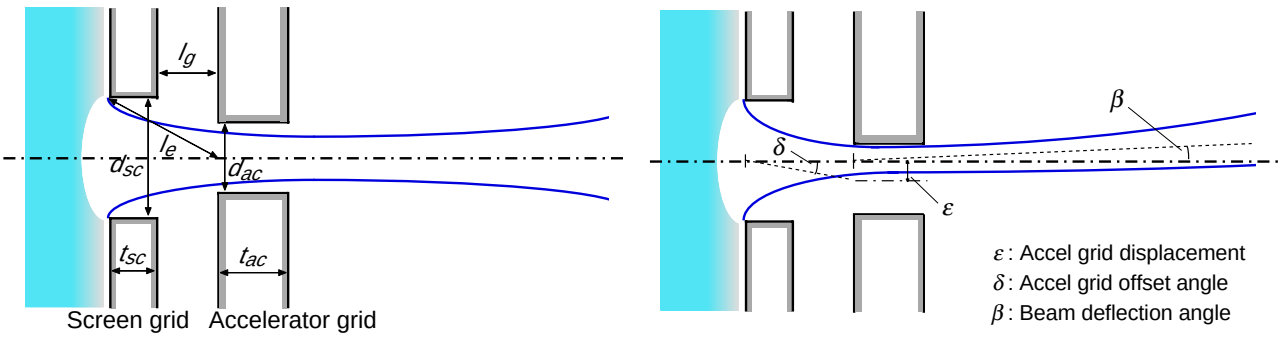

(a) Without beam deflection (b) With beam deflection

Fig. 1 Ion beam deflection by grid translation.

* okawa@nal.go.jp

dished ion optics, the translation of one of the grids without the change of grid-to-grid separation is difficult in theory.

The advances in the fabrication technology of robust carbon material such as carbon-carbon (c/c) composite in the last few decades changed the situation. Since c/c composite have almost null thermal expansion characteristics in the temperature range in practical use, flat shaped electrodes with relatively large diameter can be fabricated. These carbon electrodes are applicable to translation mechanisms for thrust vector control. Under this situation, some studies on thrust vector control of ion thrusters were started in recent years.[7,8] In addition, c/c composite is suitable for the electrodes that possess slit shaped apertures because of the selectable direction of carbon fiber weaved.[9,10] Although the thrust vectoring capability using slit type electrodes is restricted in a plane, the advantages in open area fraction capability and the facility of fabrication are still attractive.

This study was performed to explain the three dimensional behavior of deflected ion beamlets and to obtain tangible data for the design of ion optics with grid translation mechanisms. Three-dimensional and two-dimensional Particle-in-Cell simulation codes were developed to investigate the beamlet behavior both in ordinal circular apertures and slit apertures. Major issues discussed here are the effects of perveance, grid displacement directions with reference to aperture arrangement, and aperture shapes on beam deflection capability.

2. Calculation Model

The Particle-in-Cell (PIC) method was used to simulate the beamlet behavior in ion optics with grid translation mechanisms. In order to simulate the beamlet deflection phenomena both in circular and slit apertures, 2-D and 3-D codes were developed based on the IBEX-T particle simulation code[11,12] developed at Tokyo Metropolitan Institute of Technology. The computational models and the calculation process are described below.

A three-dimensional calculation is required to simulate the beamlet deflection phenomena in circular apertures because no single axis can be defined exclusively when one of electrodes is displaced laterally. Figure 2 depicts a calculation domain for ion optics with circular apertures, which was determined based on the report by Wang and Wilbur.[13] As shown in Fig. 2, the calculation domain possesses rectangular solid shape and a pair of grid holes are included in total. Using this model, it is possible to simulate the deflected beamlet behavior by moving an accelerator grid parallel to the x-axis.

One of our interest on beam deflection phenomena is the influence of the deflection direction with reference to hole arrangement. It is expected that an ion beamlet shows different behavior in deflection direction because grid holes lie in a honeycomb pattern as shown in Fig. 3. In this study, two cases of grid translation were examined: Diagonal and Parallel. The calculation domain shown in Fig. 2 was used for Diagonal translation, and the domain illustrated in Fig. 4 was used for Parallel translation. Figure 4 shows the x-y plane of the

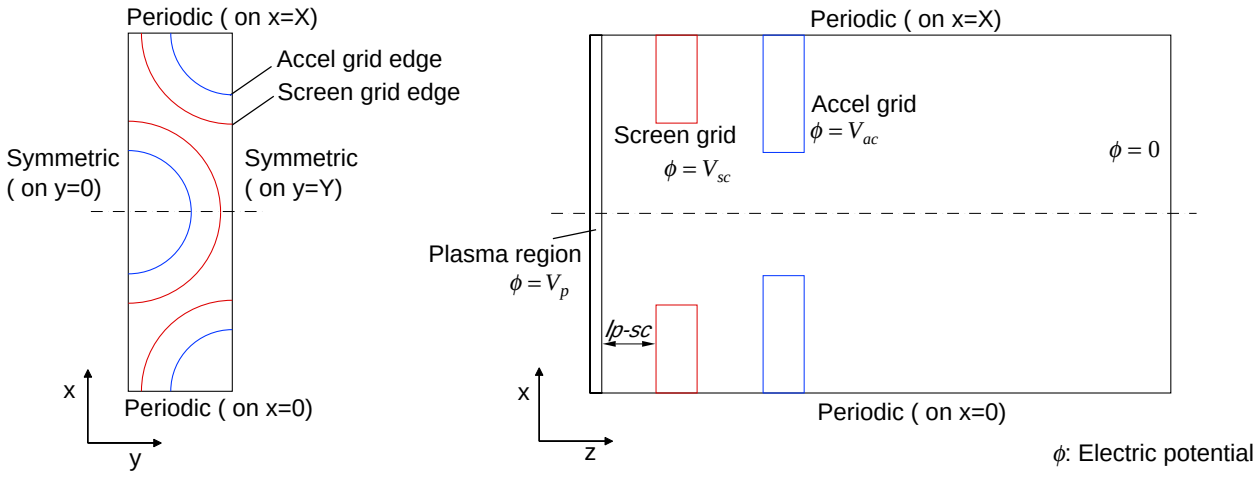

(a) x-y plane (perspective)

(b) z-x plane (y=0)

Fig. 2 Three-dimensional calculation domain for circular apertures.

domain. Using this model, the beamlet deflection phenomena parallel to the y-axis can be simulated.

In contrast with the calculation for the ion optics with circular apertures, the simulation for slit apertures is simple because a 2-D rectangular model is applicable when the existence of slit edges is neglected. Figure 5 shows the 2-D calculation domain for slit apertures. In this calculation, the open area fractions of the electrodes with slit apertures were selected equivalent to those of the circular aperture optics.

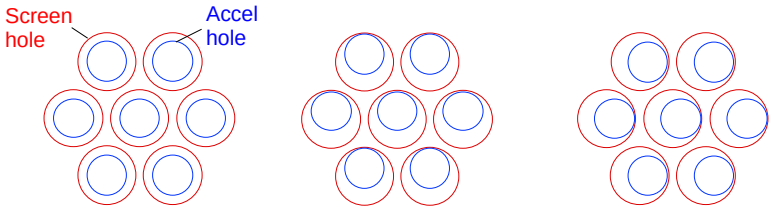

(a) No translation (b) Diagonal translation (c) Parallel translation

Fig. 3 Relationship between Accelerator grid translation direction and hole arrangement.

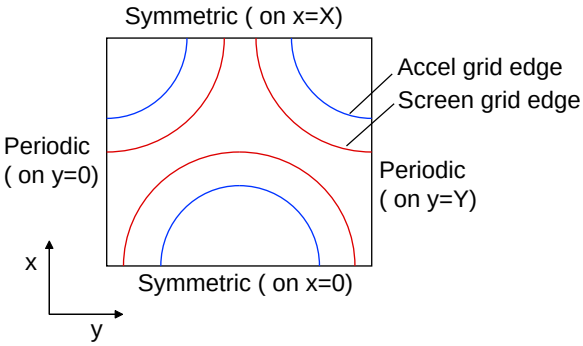

Fig. 4 x-y plane (perspective) of calculation domain for Parallel translation.

Motion of ions and electrons was calculated using the PIC method.[14] Figure 6 shows the outline of the calculation flow. As the first step, the properties of discharge-chamber plasma, grid dimensions, and applied voltages are given as input parameters. After the calculation of electrical field without any space charge, ions and electrons are generated with Maxwellian velocity distribution in the plasma region, which is placed as upstream boundary. Then the PIC routine shown in Fig. 6 is iterated until the total existing particle number becomes constant. In the PIC routine, the equations of motion of ions and electrons are solved using Euler's integration scheme, and electric field is obtained by solving Poisson's equations. A system of linear equations that consists of the Poisson's equations on each lattice is solved by the Gaussian elimination method. This matrix is refined with the consideration of potential conditions on each boundary to reduce the calculation memory and time. After the total numbers of existing particles are saturated sufficiently, the calculated total ion current (J_t – the summation of a beam current (J_b) and impingement currents to a screen grid (J_{sc}) and an accelerator grid (J_{ac})) is compared with the ion saturation current of the discharge-chamber plasma (J_{is}) that is defined by the given plasma properties. If the following equilibrium condition is satisfied, the calculation is terminated with the output.

$$J_b + J_{sc} + J_{ac} \approx J_{is} \qquad (1)$$

When the equilibrium is not satisfied, the plasma-to-screen distance ($l_{p\text{-}sc}$, illustrated in Figs. 2 and 5) is changed to lower the difference and the calculation is repeated from the first step. Details of the calculation process are described in previous papers.[11,12]

In the 3-D model for Diagonal translation illustrated in

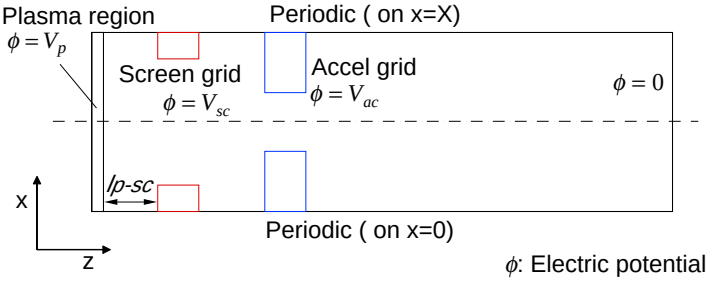

Fig. 5 Two-dimensional calculation domain for slit apertures.

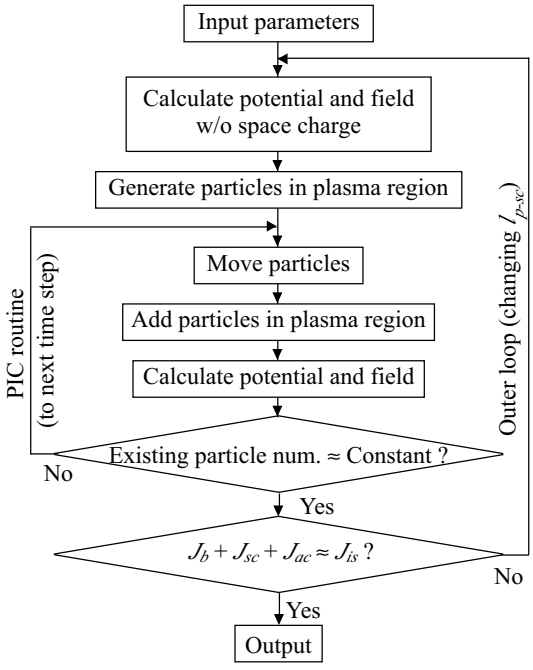

Fig. 6 Outline of calculation procedure.

Fig. 2, the domain with dimensions of (x, y, z) = (4.33, 1.25, 7.00) mm was divided into (32, 9, 70) cells. In the 3-D model for Parallel translation illustrated in Fig. 4, (2.17, 2.50, 7.00) mm domain was divided into (16, 18, 70) cells. In the 2-D model shown in Fig. 5, (x, z) = (2.17, 7.00) mm domain was divided into (50, 70) cells. The time step of the iteration was constant in 1.0×10^{-9} s in all cases. Xenon propellant was assumed to be used. Table 1 shows the input parameters.

Table 1 Input parameters.

Properties of discharge chamber plasma	
Number density, n_p, $\times10^{17}$ /m^3	0.3 ~ 3.6
Ion temperature, T_i, K	450
Electron temperature, T_e, eV	3.0
Space potential, V_p, V	1030
Accelerating voltage	
Sc grid voltage, V_{sc}, V	1000
Ac grid voltage, V_{ac}, V	-500
Grid dimensions (common)	
Sc-to-Ac separation, l_g, mm	0.8
Sc grid thickness, t_{sc}, mm	0.5
Ac grid thickness, t_{ac}, mm	0.5
Sc open area fraction, %	70
Ac open area fraction, %	33
Grid dimensions for circular apertures	
Sc hole diameter, d_{sc}, mm	2.2
Ac hole diameter, d_{ac}, mm	1.5
Hole pitch, mm	2.5
Grid dimensions for slit apertures	
Sc slit width, w_{sc}, mm	1.5
Ac slit width, w_{ac}, mm	0.7
Slit pitch, mm	2.2

3. Results and Discussions

The beamlet deflection phenomena were simulated with emphasis on the following aspects: the influences of the number density of discharge-chamber plasma, grid translation direction, and grid aperture shape (circular or slit). For the ion optics with circular apertures, the calculation models shown in Figs. 2 and 4 were used, and the model shown in Fig. 5 was used for the slit aperture case.

3-1. Standard case

A calculation result of beamlet deflection for Diagonal translation is described in this section as a typical result. In this case, the number density of discharge-chamber plasma was 3.0×10^{17} /m^3, which was equivalent to the normalized perveance per hole (*NP/H*) of 1.6×10^{-9} A/V$^{1.5}$ without grid translation. *NP/H* was defined by the following equation.

$$NP/H = \frac{J_b}{(V_p - V_{ac})^{1.5}} \frac{{l_e}^2}{{d_{sc}}^2} \tag{2}$$

Figure 7 shows ion particle distributions and electric potential contours on y=0 plane in Fig. 2 at the grid offset angle of 0, 5.9, 11.8, 17.3, and 22.6 °. These offset angles correspond to the accelerator grid translation distances of 0, 0.14, 0.27, 0.41, and 0.54 mm respectively – these are dominated by the calculation mesh size. In Fig. 7, the ion beamlets are tilted upward by displacing the accelerator grid downward. Also observed is that the ion impingement to the accelerator grid is not significant when the offset angle is below 11.8 °.

Beamlet deflection angles and the ratio of an accelerator grid current to a beam current (J_{ac}/J_b) as a function of the grid offset angle are shown in Figs. 8 and 9 respectively. The beam deflection angle is defined in Fig. 1. In the calculation, the beamlet deflection angle was calculated by measuring the displacement distance of the center of the beamlet at 3.0 mm downstream from the accelerator grid. The beamlet center was defined as the position where the number of beam ions was divided in half. As shown in Fig. 8, the beamlet deflection angle is almost proportional to the grid offset angle. The proportionality constant is approximately 0.4 in this case. Figure 9 illustrates that the impingement current to the accelerator grid rises abruptly at the impingement limit (approximately 15 °). These tendencies agree well with the experimental results reported in other studies.[4,8]

3-2. Effect of number density of discharge-chamber plasma

The influence of the number density of discharge-chamber plasma on beamlet deflection capability should be investigated because the plasma number density is not constant in a discharge-chamber in practical use. Figure 10 shows the beamlet deflection angles plotted against the grid offset angle when the plasma number density is 1.5 and 3.0×10^{17} /m^3. Each number density corresponds to *NP/H* of 0.9 and 1.6×10^{-9} A/V$^{1.5}$ respectively when the accelerator grid current is negligible. Figure 10 indicates that the beamlet has larger deflection angles with smaller plasma number densities at equivalent offset angles. In the case with the number density of 1.5×10^{17} /m^3, the deflection angle is approximately 1.5 times as large as that with the number density

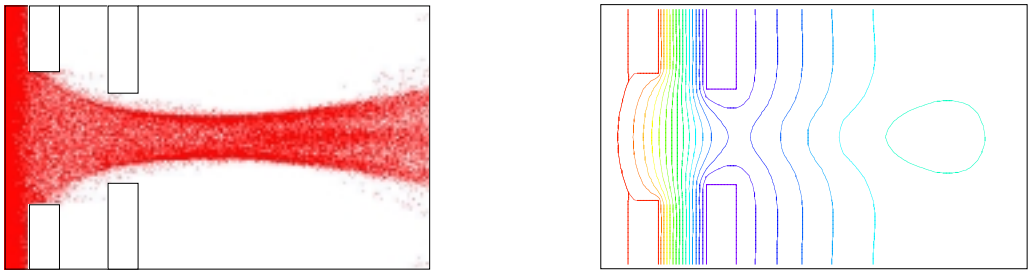

(a) Grid offset angle of 0 ˚

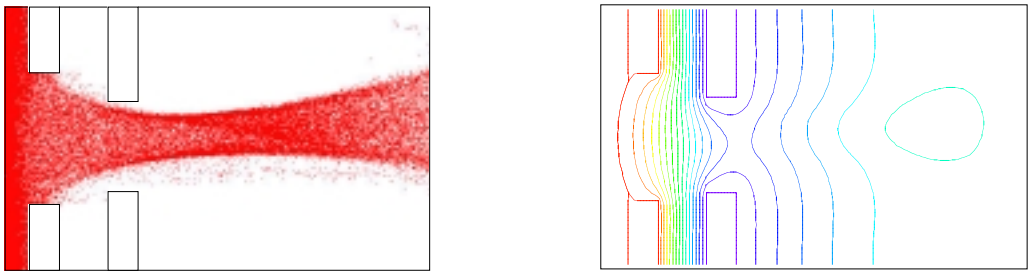

(b) Grid offset angle of 5.9˚

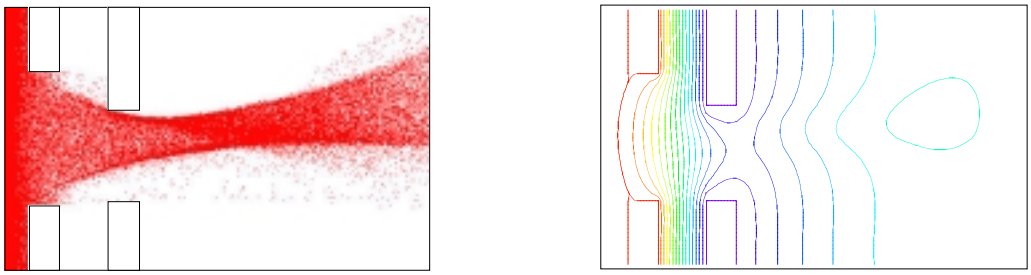

(c) Grid offset angle of 11.8 ˚

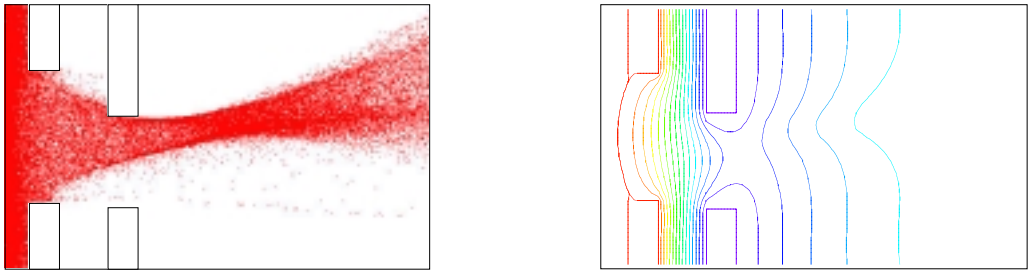

(d) Grid offset angle of 17.3 ˚

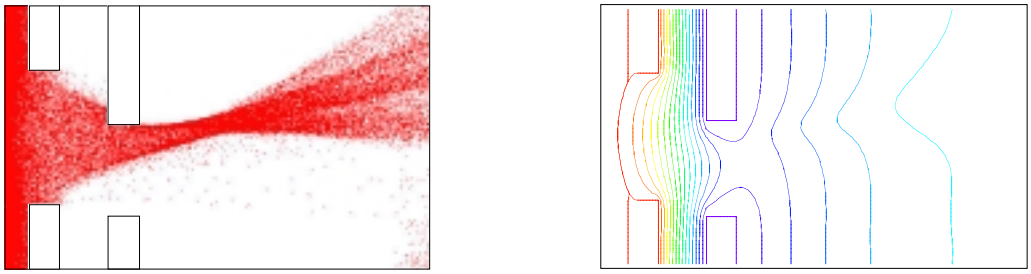

(e) Grid offset angle of 22.6 ˚

Fig. 7 Ion particle distribution and electric potential contours on y=0 plane at each grid offset angle for Diagonal translation. (Potential contours: from -500 V to 1000 V at 100 V interval.)

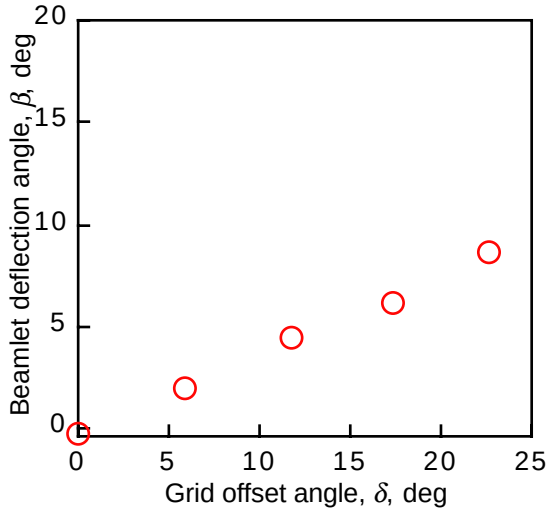

Fig. 8 Beamlet deflection angle vs. grid offset angle in standard case.

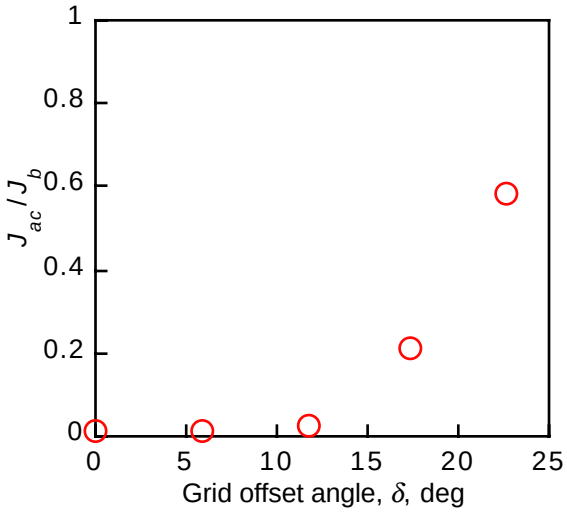

Fig. 9 Ratio of accelerator grid current to beam current vs. grid offset angle in standard case.

of 3.0×10^{17} /m^3. Linear relations between deflection and offset angles are observed independently of the number density.

The ratios of the accelerator grid current to the beam current in the two number density conditions at various offset angles are shown in Fig. 11. Abrupt increase in the accelerator grid current at a certain point of the grid offset angle is observed in both cases, however, the impingement limit angle strongly depends on the number density. When the number density is 1.5×10^{17} /m^3, the acceptable offset angle with the negligible accelerator grid current is larger than that with the number density of 3.0×10^{17} /m^3 by a factor of 1.5. Similar trend has been reported in other report.[4] These results indicate that the beamlet deflection angle is not constant along a radius of a discharge-chamber because the plasma number density is not constant either in practical use.

3-3. Effect of grid translation direction

As shown in Fig. 3, it is anticipated that beam deflection capability is affected by the relationship between the grid translation direction and the grid hole arrangement. In order to investigate this issue, the beam deflection phenomena for Diagonal and Parallel translation described in Fig. 3 were compared with each other. Figure 12 shows the ion particle distribution and the potential contours in both cases when the grid offset angle is approximately 12 ˚. In Fig. 12 (b), the ion distribution and potential profile on the x=0 plane (shown in Fig. 4)

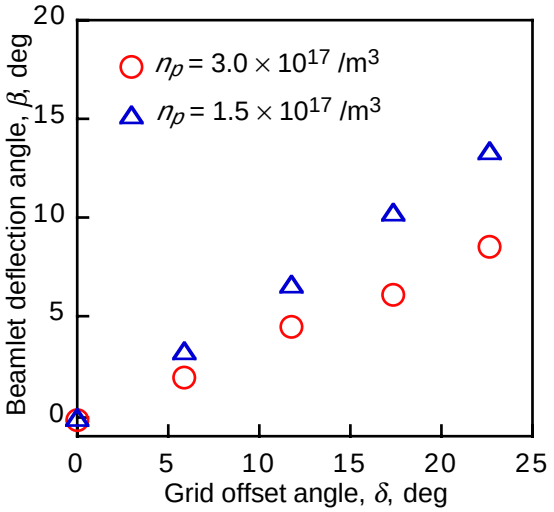

Fig. 10 Beamlet deflection angle vs. grid offset angle in discharge plasma number densities of 3.0 and 1.5 $\times 10^{17}$ /m^3 cases.

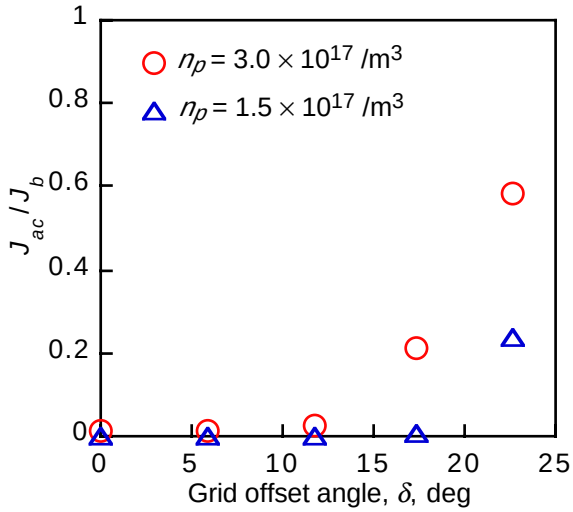

Fig. 11 Ratio of accelerator grid current to beam current vs. grid offset angle in discharge plasma number densities of 3.0 and 1.5 $\times 10^{17}$ /m^3 cases.

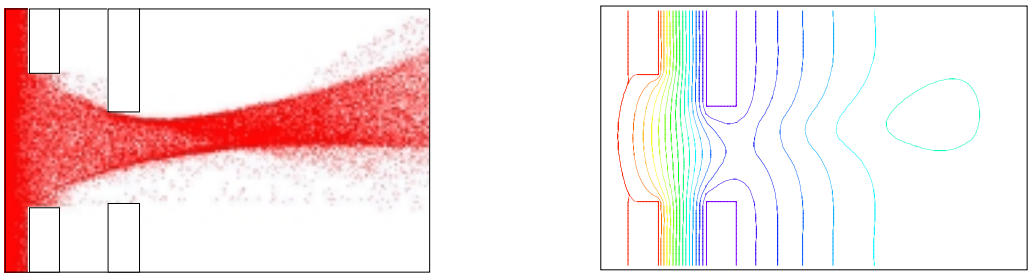

(a) Diagonal translation (same as Fig. 7 (c))

(b) Parallel translation

Fig. 12 Ion particle distribution and electric potential contours for Diagonal (on y=0 plane) and Parallel (on x=0 plane) translation at grid offset angle of approximately 12 ˚. (Potential contours: from -500 V to 1000 V at 100 V interval.)

are depicted. Figure 12 indicates that there are little differences in beamlet shape and potential profile between Diagonal and Parallel translation. The appearance of ion particles near the lower right corner in Fig. 12 (b) is attributable to the small hole-to-hole distance on this plane and this difference does not mean the difference in phenomenon. The beam deflection angle and J_{ac}/J_b as a function of the grid offset angle for both cases are shown in Figs. 13 and 14 respectively. Both figures indicate that there are almost no differences in beam deflection angles and grid impingement currents between Diagonal and Parallel translation.

The obtained results show that the influence of the relative position of grid apertures on beam deflection capability is negligible within the practical grid offset range with an acceptable impingement current. Therefore it is said that there is no need to consider the influence of hole arrangement to design the ion optics for thrust vectoring.

3-4. Slit aperture optics

The calculation for slit aperture optics was conducted using the 2-D rectangular model shown in Fig. 5. The slit widths of the screen and accelerator grid were selected to have equivalent open area fractions to the circular aperture grids. The number density of discharge-chamber plasma was selected at 3.6×10^{17} /m^3. The

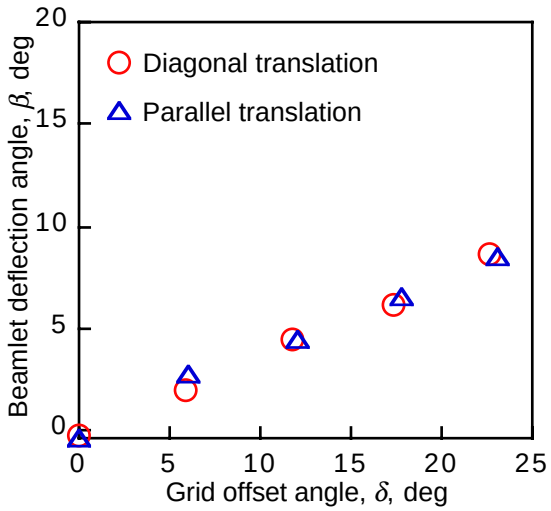

Fig. 13 Beamlet deflection angle vs. grid offset angle for Diagonal and Parallel translation.

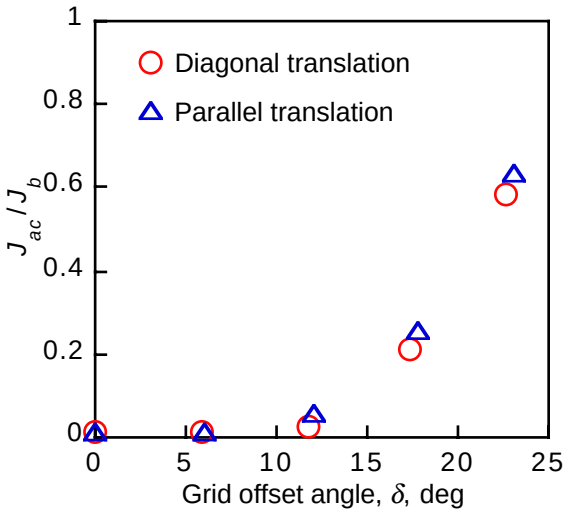

Fig. 14 Ratio of accelerator grid current to beam current vs. grid offset angle for Diagonal and Parallel translation.

difference from the above-described standard case in the number densities exists because the adjustment of the number density was required to satisfy the current equilibrium condition of Eq. (1).

Figures 15 and 16 show the beam deflection angle and J_{ac}/J_b plotted against the grid offset angle for the slit and the circular aperture optics, respectively. Data for circular aperture optics is equivalent to those in Figs. 8 and 9. Figure 15 illustrates that the inclination of the beam deflection curve against the offset angle for the slit aperture optics is approximately twice as that for circular aperture optics. This result means that larger beam deflection angles can be obtained with smaller grid translation in slit aperture optics compared with the ordinal circular aperture case. On the other hand, the grid offset angle with the sharp increase in the accelerator grid current for the slit aperture optics is smaller than that of the ordinal optics. In addition, the rise in the accelerator grid current for the slit optics is so abrupt that no ion beam is extracted over 12 ˚ of the grid offset angle.

From Figs. 15 and 16, it is estimated that the available beam deflection angle limit, under which the impingement current is not significant, and the grid offset angle at that time are approximately 10 ˚ and 10 ˚ respectively for the slit optics and approximately 5 ˚ and 13 ˚ respectively for the circular aperture optics. This comparison indicates that ion optics with slit apertures is useful for thrust vectoring if there is a requirement of thrust vector control in a plane. Here, it should be noted that the beam divergence angle for the slit optics is approximately 25 % larger than that for the ordinal optics though the tangible data are not described in this paper. From another point of view, the slit aperture optics with grid translation mechanisms are useful for ground application because larger beam deflection angles and beam divergency are suitable to form uniform ion flux in large area. It is also said that the precise alignment in grid position and shape is required to extract an on-axis sheet beam because the optics with slit apertures is sensitive in beam deflection.

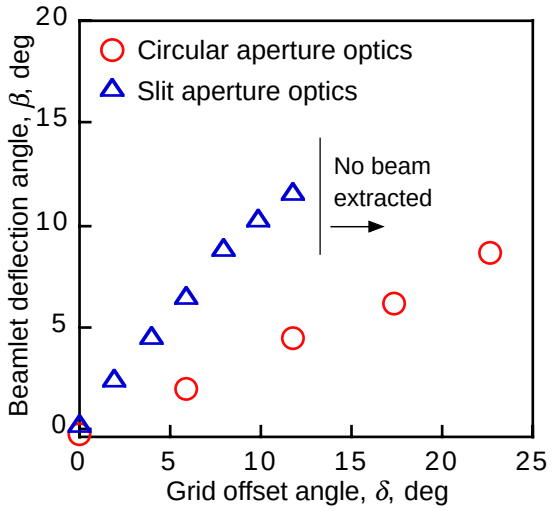

Fig. 15 Beamlet deflection angle vs. grid offset angle for circular and slit aperture optics.

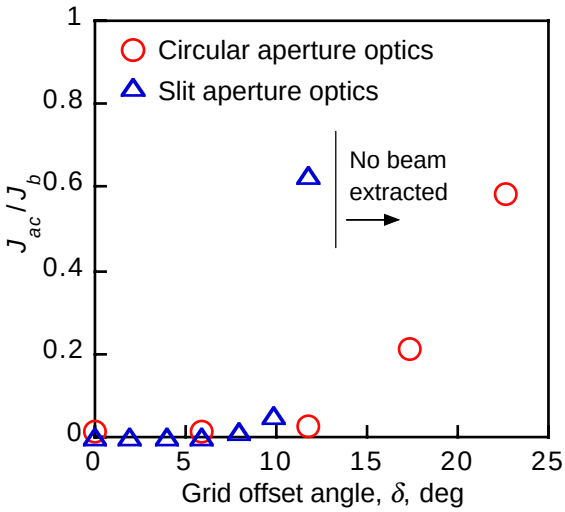

Fig. 16 Ratio of accelerator grid current to beam current vs. grid offset angle for circular and slit aperture optics.

4. Future Work

From the calculation results described above, useful information was obtained to design the thrust vectoring mechanism by grid translation. However, there still remain some parameters to be considered, which are necessary to determine the grid dimensions and operating conditions. In addition, the calculation code developed has not been sophisticated at present especially in the linear equations solver. In order to treat a larger amount of calculation meshes, the improvement of the simulation code is necessary. Besides, we plan to conduct the experiment of ion beam steering in near future.

5. Summary

The numerical simulation of ion beamlet deflection phenomena correspondence to thrust vectoring by grid translation was performed. The three-dimensional and two-dimensional Particle-in-Cell simulation codes were developed to calculate the beamlet behavior in ordinal circular aperture optics and slit aperture optics. The simulation codes feature rectangular solid calculation domains and self-consistent ion sheath formation. The obtained results indicated that 1) a beam deflection angle is proportional to a grid offset angle and the inclination strongly depends on the number density of discharge-chamber plasma, 2) the grid displacement direction with reference to grid aperture arrangement has slight influences on beam deflection capability, 3) ion optics with slit apertures obtain larger beam deflection angles with smaller grid displacement compared with those of ordinal circular aperture optics. The obtained results are useful to design the ion optics with grid translation mechanisms for thrust vector control.

References

1. Anderson, J. R. and Work, G. A., "Ion Beam Deflection for Thrust Vector Control," 5th Electric Propulsion Conference, AIAA-66-204, 1966.
2. Fosnight, V. V., Dillon, T. R., and Sohl, G., "Thrust Vectoring of Multiaperture Cesium Electron Bombardment Ion Engines," J. Spacecraft and Rockets, Vol. 7, No. 3, 1970, pp. 266-270.
3. Lathem, W. C., "Grid-Translation Beam Deflection Systems for 5-cm and 30-cm Diameter Kaufman Thrusters," 9th Electric Propulsion Conference, AIAA-72-485, 1972.
4. Homa, J. M. and Wilbur, P. J., "Ion Beamlet Vectoring by Grid Translation," 16th International Electric Propulsion Conference, AIAA-82-1895, 1982.
5. Hayakawa, Y., "Three-Dimensional Numerical Model of Ion Optics System," J. Propulsion and Power, Vol. 8, No. 1, 1992, pp. 110-117.
6. Tartz, M., Hartmann, E., Deltschew, R., and Neumann, H., "Thrust-Vector Tilting Caused by Grid Misalignment," 27th International Electric Propulsion Conference, IEPC-01-114, 2001.
7. Fearn, D. G., "Ion Thruster Thrust Vectoring Requirements and Techniques," 27th International Electric Propulsion Conference, IEPC-01-115, 2001.
8. Haag, T., "Translation Optics for 30 cm Ion Engine Thrust Vector Control," 27th International Electric Propulsion Conference, IEPC-01-116, 2001.
9. Meserole, J. S. and Rorabaugh, M. E., "Fabrication and Testing of 15-cm Carbon-Carbon Grids with Slit Apertures," 31st Joint Propulsion Conference, AIAA-95-2661, 1995.
10. Brophy, J. R., Mueller, J., and Brown, D. K., "Carbon-Carbon Ion Engine Grids with Non-Circular Apertures," 31st Joint Propulsion Conference, AIAA-95-2662, 1995.
11. Okawa, Y. and Takegahara, H., "Numerical Study of Beam Extraction Phenomena in an Ion Thruster," Japanese J. Applied Physics, Vol. 40, Part 1, No. 1, 2001, pp. 314-321.
12. Okawa, Y., Takegahara, H., and Tachibana, T., "Numerical Analysis of Ion Beam Extraction Phenomena in an Ion Thruster," 27th International Electric Propulsion Conference, IEPC-01-097, 2001.
13. Wang, J., Polk, J., Brophy, J., and Katz, I., "3-D Particle Simulation of NSTAR Ion Optics," 27th International Electric Propulsion Conference, IEPC-01-085, 2001.
14. Birdsall, C. K. and Langdon, A. B., "Plasma Physics via Computer Simulation, Inst. Phys. Publishing, Bristol, 1991.